AMERICAN UNIVERSITY OF BEIRUT

OPTIMIZING PERFORMANCE OF CEILING MOUNTED PERSONALIZED VENTILATION SYSTEM ASSISTED BY CHAIR FANS: ASSESSMENT OF THERMAL COMFORT AND INDOOR AIR QUALITY

by
BACHIR KHALED EL FIL

A thesis
submitted in partial fulfillment of the requirements
for the degree of Master of Engineering
to the Department of Mechanical Engineering
of the Faculty of Engineering and Architecture
at the American University of Beirut

Beirut, Lebanon
July 2015

AMERICAN UNIVERSITY OF BEIRUT

OPTIMIZING PERFORMANCE OF CEILING MOUNTED PERSONALIZED VENTILATION SYSTEM ASSISTED BY CHAIR FANS: ASSESSMENT OF THERMAL COMFORT AND INDOOR AIR QUALITY

by
BACHIR KHALED EL FIL

Approved by:

Dr. Nesreen Ghaddar, Professor — Advisor
Department of Mechanical Engineering, AUB

Dr. Kamel Ghali, Professor — Member of Committee
Department of Mechanical Engineering, AUB

Dr. Fadl Moukalled, Professor — Member of Committee
Department of Mechanical Engineering, AUB

Date of thesis/dissertation defense: July 20, 2015

AMERICAN UNIVERSITY OF BEIRUT

THESIS, DISSERTATION, PROJECT RELEASE FORM

Student Name: El Fil Bachir Khaled
Last First Middle

● Master's Thesis ○ Master's Project ○ Doctoral Dissertation

☑ I authorize the American University of Beirut to: (a) reproduce hard or electronic copies of my thesis, dissertation, or project; (b) include such copies in the archives and digital repositories of the University; and (c) make freely available such copies to third parties for research or educational purposes.

☐ I authorize the American University of Beirut, **three years after the date of submitting my thesis, dissertation, or project,** to: (a) reproduce hard or electronic copies of it; (b) include such copies in the archives and digital repositories of the University; and (c) make freely available such copies to third parties for research or educational purposes.

Signature

July 28, 2015

Date

ACKNOWLEDGMENTS

Scientific research requires a lot of commitment of both time and effort to come up with a successful research work. Therefore, this thesis work is not the fruit of an individual effort and it could not have been achieved without the support and assistance of many persons. For that reason, I would like to thank a few.

I would like to thank my advisors at the American University of Beirut for their continuous support and guidance throughout my research work. I acknowledge the effort of Dr. Nesreen Ghaddar and Dr. Kamel Ghali for their original involvement and guidance, and motivation which contributed a lot to this thesis.

I would like also to thank my committee member, Dr. Fadl Moukalled for his attendance and guidance especially in the numerical simulations. I would like to thank all staff and faculty members of the American University of Beirut for their great help and patience, which contributed a lot to the smooth achievement of my thesis.

I would like to express cordial gratitude to my friends and colleagues at the American University of Beirut who without them I would not have been able to achieve what I have reached in particular Nagham Ismail, Carine Habchi, Sylvie Antoun, Walid Abou Hweijj, and Rami Bitar.

Also I express great thanks to my dearest friends and family (Father, Mother, and my sisters) for their patience and continuous unconditional support.

AN ABSTRACT OF THE THESIS OF

Bachir Khaled El Fil for Master of Engineering
Major: Mechanical Engineering

Title: Optimizing performance of ceiling Mounted personalized ventilation system assisted by chair fans: assessment of thermal comfort and indoor air quality

This study investigates and optimizes the performance of ceiling mounted personalized ventilation (*PV*) system when assisted with chair-mounted fans. Detailed computational fluid dynamics (CFD) simulations were performed to study the velocity, temperature, and CO_2 fields around the microclimate of the occupant. The CFD model was integrated with a bioheat model to determine the corresponding segmental skin temperature and local and overall comfort and sensation. The CFD model was validated experimentally using a thermal manikin in a climatic chamber. Segmental skin temperature, velocity field, and CO_2 field were validated experimentally. The predicted values and the measured values showed good agreement.

The validated CFD model was used to optimize the height of chair-fan and the fan flow rate for the best combination of indoor air quality and thermal comfort. The chair fans configuration to achieve best thermal comfort and best IAQ occurred at different fan heights. The optimal fan height and flow rate for best thermal comfort were 40 cm above floor level and 10 L/s, respectively. However, the optimal fan height and flow rate for best air quality were found to be 50 cm above the floor level and 10 L/s, respectively. At this configuration, the chair-mounted-fans were able to reduce the thermal plumes and improve the performance of the PV system by nearly doubling thermal comfort and ventilation effectiveness. The use of chair mounted fans permitted achieving energy savings up to 17% when compared with conventional mixing ventilation system.

CONTENTS

ACKNOWLEDGEMENTS..... v

ABSTRACT..... vi

LIST OF ILLUSTRATIONS..... xi

LIST OF TABLES..... xiii

LIST OF ABBREVIATIONS..... xiv

Chapter

1. INTRODUCTION..... 1

1.1. Thesis Objective 5

2. SYSTEM DESCRIPTION..... 6

3. METHODOLOGY 7

3.1. CFD modeling 10

3.1.1. Air flow modeling 10
3.1.2. Air quality modeling 15
3.1.3. Bioheat model..... 17

3.2. Experimental Protocol..... 19

3.3. Parametric Study..... 23

4. RESULTS AND DISCUSSIONS..... 25

4.1. CFD Validation..... 25

4.2. Parametric Study..... 29

4.2.1. Air quality comparison……... 30
4.2.2. Thermal Comfort…….. 33

4.2.3. Energy Analysis…….. 39

4. CONCLUSION AND RECOMMENDATIONS……. 42

Appendix

BIBLIOGRAPHY..... 44

ILLUSTRATIONS

Figure		Page
1.	Schematic diagram of the proposed system.....	6
2.	Schematic diagram of the (a) chair mechanism (b) top view (c) front view…….	8
3.	(a)The computational domain used in the simulations (b) the generated grid.....	11
4.	Flow chart showing the algorithm for coupling between CFD and Bioheat model.....	18
5.	(a) The thermal manikin that was used in the experiment (b) the chair fan mechanism.....	20
6.	Thermocouples distributed over the segmental parts of the thermal manikin, the thermal manikin‘s representation is a default dummy in the commercial CFD software ANSYS.....	22
7.	PV nozzle jet validation and turbulence intensity as function of distance away from the nozzle.....	26
8.	The measured and the predicted ventilation effectiveness at the breathing zone for a single PV system having fresh flow rate of 7.5 L/s and T = 16 ℃ and total fan flow rate of 10 L/s.....	27
9.	Segmental Skin validation: (a) Fans OFF (b) Fan H=30 cm (c) Fan H=40cm (d) Fan H=50 cm; at Q = 10 L/s.....	28
10.	Overall comfort and Ventilation effectiveness as function of total fan flow rate at fan level (a) 30 cm (b) 40 cm (c) 50 cm…….....	32
11.	Overall (a) comfort and (b) sensation for different fan configuration.....	33
12.	Displays the contour plots of (a) velocity, (b) temperature, (c) CO_2 concentration fields at a selected case having fan height of 40 cm and a total fan flow rate of 10 L/s.....	38
13.	The normalized shift of thermal comfort and IAQ as function of fan height at a constant total fan flow rate of 10 L/s……	40

TABLES

TABLE		PAGE
1	Boundary Conditions and Schemes used in the Simulations……	13
2	The grids used for mesh independency……	15
3	The conducted experiments used for model validation……	22
4	Simulation Cases used in the parametric study ……	24
5	Model Validation: The near head velocity and temperature of the measured values versus predicted values by CFD model for case of PV jet of 7.5 L/s and temperature of 16℃……	28
6	Comparison of the ventilation effectiveness, near head velocity, and near head temperature having chair fans fixed at height of 30 cm, 40 cm, and 50 cm at different fan flow rates, PV jet having 8.5 L/s……	34
7	Segmental thermal comfort and Sensation for the selected cases at fan height of 40 cm……	37

CHAPTER I

INTRODUCTION

Indoor air quality and thermal comfort are two critical factors that researchers focused on because they have a direct influence on the occupants' health and performance. People living in urban regions spend more than 90% of their time in closed indoor spaces [1]. The energy consumption in the building sector accounts for 50% of the total worldwide energy produced. In an effort to reduce the building energy consumption and the resulting carbon emissions responsible for the global warming of the environment, scientists have researched three areas in their studies of energy efficient buildings: the building envelope material, efficiency of the air-conditioning system devices and the use of hybrid air-conditioning systems powered partially/totally by renewable energy resources.

These indoor spaces must be conditioned to provide the occupants' thermal needs. The thermal environment and air quality in any indoor room is not always optimal for energy conservation goals. Ventilation systems will condition i.e. heat or cool the indoor space to provide thermal comfort and to evacuate contaminants that are generally generated by occupants, building material, or furniture. The effort to come up with an

energy efficient system for heating, ventilation and air conditioning (HVAC) has been the trend in current building design.

One of the commonly used methods for energy efficient systems is by localizing thermal comfort and indoor air quality [2-12]. Localizing thermal comfort and indoor air quality is only viable via complex systems. Moreover, confining thermal comfort and air quality tends to reduce energy consumption because it directly supplies conditioned air to the breathing zone (i.e. minimizing the entrainment with the recirculated air) of the occupant rather than having it supplied via diffusers in the conditioned space. Lately, the use of *PV* systems has become the trend to provide the occupant's local needs while maintaining low energy consumption. Melikov et al. [6] investigated the use of different types of *PV* systems and reported remarkable enhancement for thermal comfort and indoor air quality. For instance, personalized task ventilator systems that require underfloor air distribution systems are used commonly in office spaces since this system does not need any exposed ducting [2]. However these technologies are expensive, their payback period is uncertain, and it is difficult to retrofit these systems to existing air distribution units.

To overcome all these challenges, Yang et al. [13] suggested the integration of ceiling mounted personalized systems to conventional mixing ventilation system in order to eliminate the need to extend ducts. Yet, the promising ceiling mounted

ventilation system had limited success. In principle, the fresh jet supplied by the ceiling mounted *PV* system should be capable of reaching breathing zone of the occupant with minimal entrainment of the contaminated room air, and it should have a sufficient near head velocity of at least 0.3 m/s [15-17] so that it is able to penetrate the occupant's rising convective plume. Melikov et al [12] studied the benefit of air flow interaction control in the microclimate of the occupant aiming to enhance thermal comfort and indoor air quality. In a ceiling mounted personalized ventilation system, shear stress arising between the fresh air and the existing contaminated room air plays a major role in reducing the effectiveness of the system. Khalifa et al [18, 19] investigated the performance of desk personalized coaxial *PV* system and reported an improved performance by delivering fresh effectively to the breathing zone of the occupant. Moreover, Bolashikov [9, 10] showed that the use of desk mounted fans was successfully able to control the convective plume arising from the occupant and therefore delivering more fresh air horizontally. To solve the problem of the ceiling mounted *PV* system, Makhoul et al. [15] proposed a ceiling mounted coaxial nozzle where the primary nozzle supplies fresh air surrounded by concentric secondary nozzle supplying return air at the same velocity. Makhoul et al. [15-16] reported an enhancement of 3-4 times better ventilation effectiveness when using coaxial nozzle compared to conventional nozzle supplying the same amount of fresh air. Nevertheless,

one of the major drawbacks of the coaxial system is that it is more complex to operate, design, and to retrofit into existing nozzles. Therefore, it is of interest to find other means by which the simple *PV* jet system can be modified without any additional complexities in the system design.

Makhoul et al. [17] have used desk mounted fans to enhance the effectiveness of *PV* system, which was proposed by Yang et al [13], by controlling the convective flow around the occupant using desk suction fan thus hindering free convection. Installing desk-mounted fans as an option to control the convective plumes generated by the human body showed a good performance for enhancement potential. However, the success of the desk fans in suppressing the human thermal plumes is limited. It is effective only when the occupant is close to the desk. Chair fans offer a more promising solution since they are attached to the chair, and therefore they will pull down the thermal plumes regardless of the person's position.

Previous researchers have tackled the importance of chair fans for an individually controlled comfort [20]. Habchi et al. [21] investigated empirically the effect of chair fans along with *DV* system; however the challenge is in the case of the downward jet. No work has been reported in the literature to address the use of chair fans to enhance the performance of the ceiling mounted *PV* system with optimization. Nonetheless, when it comes to implementing chair fans to assist the single jet *PV* system, two

parameters play a major role in determining the local comfort, sensation, and ventilation effectiveness at the breathing zone of the occupant. These parameters are (i) the elevation of the fans i.e. height at which they are fixed on the chair and (ii) the flow rate at which the air is being sucked by the fan. Having the fans at a really high level above the ground will for sure enhance IAQ, since the fans will allow the fresh air jet to reach breathing zone of the occupant effectively, before it entrains recirculated air. However, this fresh air jet might cause local discomfort on the head and upper body segments since it might have higher velocity at lower temperature. On the other hand, placing the fans at a relatively low height will cause the fresh air to entrain more recirculated air, thus the air quality may not be as good as that when placing the fans at a higher level, but the temperature of the air jet might be warmer since it is mixed with the recirculated air. Optimizing the height of the chair fans with respect to indoor air quality may not simultaneously be the optimal setting to maintain thermal comfort at these conditions for minimal energy consumption.

Therefore, the objective of this work is to find the optimal height and the total flow rate of the chair fans that will result in attaining the best combination of thermal comfort and indoor air quality. This paper investigates by modeling and experimentation the enhancement in the performance of ceiling mounted single jet *PV* nozzle placed at the center of the supply diffuser when assisted by chair fans for controlling the natural

plumes generated by human body.

Computational fluid dynamics (CFD) simulations will be performed for determining the microclimate velocity, temperature, and CO_2 concentration fields. In addition, the 3D-CFD model will be integrated with a bioheat model to help in obtaining the segmental and overall comfort and sensation, and the segmental skin temperature. Moreover, experiments will be conducted on a thermal manikin to validate the thermal and flow field and air quality around the manikin as measured by the CO_2 sensors. This will be followed by a parametric study to determine the best combination of fan's height and fan flow rate that will attain best indoor air quality and thermal comfort at minimum energy. The novel optimized system will be compared to the conventional mixing ventilation system. The comparison will be based on attaining the same local and overall thermal comfort and ventilation effectiveness.

1.1. Thesis Objectives

In this Master's thesis, an investigation of the performance and applicability of the personalized ventilation systems to be assisted by chair fans is accessed for indoor air quality and thermal comfort. In addititon, the feasible system (PV+CF) will be then optimized to achieve lowest energy consumption. Since any mathematical modeling of the system is complex, CFD modeling was used. CFD simulations on ANSYS Fluent

are used mainly to capture the velocity and thermal fields in addition to the concentration field of carbon dioxide in an office space [15-17, 21, 22]. The 3D CFD model is integrated with a validated bioheat model [23, 24]. The bio heat model is used mainly to assess localized thermal comfort and sensation that are attained by the occupant under specific PV parameters. Salloum et al. [23] bioheat model and Zhang et al. [25-27] comfort models are integrated in the CFD model to predict the segmental skin temperature for the CFD model and the segmental comfort and sensation. The findings of the CFD simulation are then validated experimentally. The experiments are conducted on a thermal manikin seated under the diffuser in the center of the room.

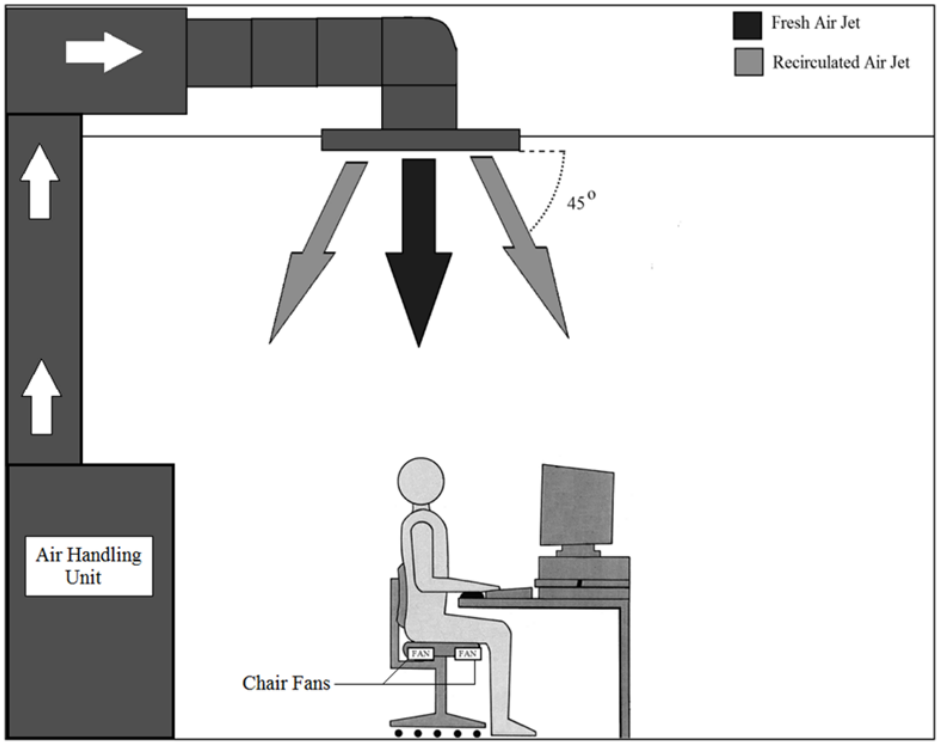

Figure 1- Schematic diagram of the proposed system

CHAPTER II

SYSTEM DESCRIPTION

The localized HVAC system under consideration is depicted in Fig. 1-1 and is composed of an air distribution system i.e. ceiling mounted personalized ventilation system, and beneath it directly an office chair mounted with fans. The air distribution system consists of a single nozzle that supplies fresh air to provide the occupant with breathable air of high quality, and four peripheral diffusers that supply recirculated air at an angle of 45°. These angled diffusers permit the formation of a canopy effect around the occupant, thus helping in confining the flow. The canopy will allow maintaining a desired air temperature in the microclimate of the occupant lower than that of the macroclimate air temperature. In addition, the chair mounted fans are placed on each side supplying uniform flow rate. The fans have a single degree of freedom mechanism, in which they are allowed to move up-and-down vertically. Fig. 2 shows how the fans are fixed on the chair; moreover it shows the distances at which the fans are set. Only two parameters are considered for optimization, the fan flow rate $\left(\dot{Q}_f\right)$ and fan height $\left(H\right)$. On the other hand, the carbon dioxide gas, which is used as a tracer

gas in this study, is injected to the room through a tube to mimic a typical CO_2 flow rate in an office space.

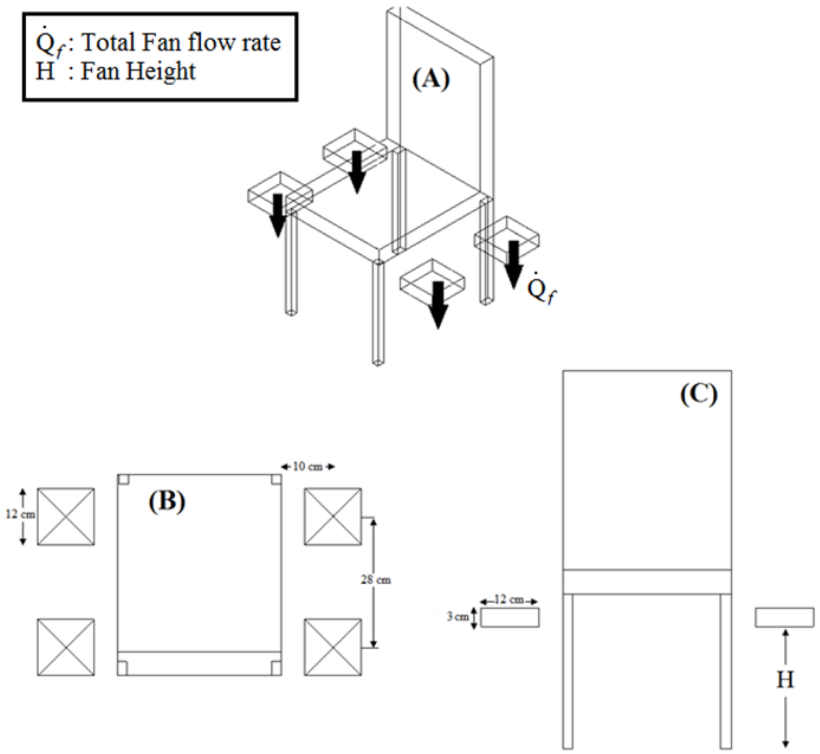

Figure 2- Schematic diagram of the (a) chair mechanism (b) top view (c) front view

CHAPTER III

METHODOLOGY

The objective of the proposed fan-equipped chair combined with ceiling mounted personalized ventilation system is to control the convective flow resulting from the rising plumes of the occupant and to find an optimal height and flow rate for the chair fans to ensure good indoor air quality and thermal comfort at minimal energy consumption. The relatively complex interaction occurring between the rising thermal plumes and the ceiling mounted *PV* jet acting downwards rendered the modeling process more complicated, therefore the CFD simulation will be used to capture the intricate interaction between the rising plumes, *PV* downward jet, and the chair fans. Therefore to assess the performance of the proposed system in maintaining localized thermal comfort and air quality, 3D-CFD simulations will be performed using the commercial software ANSYS Fluent© [22].

CFD simulations on ANSYS Fluent are used mainly to capture the velocity and thermal fields in addition to the concentration field of carbon dioxide in an office space [15-17, 21, 22]. The 3D CFD model is integrated with a validated bioheat model [23, 24]. The bio heat model is used mainly to assess localized thermal comfort and

sensation that are attained by the occupant under specific *PV* parameters. Salloum et al. [23] bioheat model and Zhang et al. [25-27] comfort models are integrated in the CFD model to predict the segmental skin temperature for the CFD model and the segmental comfort and sensation. The findings of the CFD simulation are then validated experimentally. The experiments are conducted on a thermal manikin seated under the diffuser in the center of the room.

Since this study is targeting two main aspects; thermal comfort and indoor air quality in non-residential spaces, a full scale computational domain representing a typical office workspace is adopted as shown in Fig 3a. At the same level of thermal comfort and ventilation effectiveness, the optimized system will then be compared to the conventional mixing ventilation in terms of energy savings, which will be tackled later in the results and discussion.

3.1 CFD Model

Coupling the *PV* system with chair fans will induce complex flow interaction between the air-jets present in the room. The fans are sucking the rising thermal plume, while the nozzle is supplying a vertical jet of fresh air to the office space. CFD modeling has shown to be very effective in capturing the physics of complex flow problems; moreover CFD modeling has shown good prediction of the air flow pattern and species

distribution in the space for different HVAC configurations [28, 29]. Hence CFD is a suitable tool to investigate the performance of the ventilation system in an indoor environment, and it is used in this work to study the performance of coupling the *PV* system with chair fans. Moreover, since there exist no high temperature gradient in the conditioned space, radiation is neglected in this study for its insignificant effect.

3.1.1 Airflow modeling

A detailed 3D-CFD model (as shown in Fig. 3a) was developed to accurately predict the air entrainment by the rising convective thermal plume and their interaction with suction jets due to chair fans. To attain robust CFD results, it is essential to model the physics of the flow i.e. the turbulence, buoyancy, and boundary layers near surfaces.

(a)

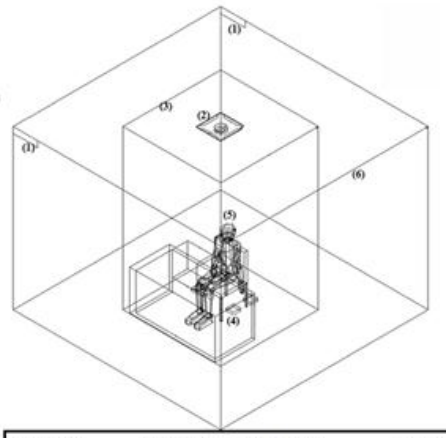

(1) Exhaust	(2) Ceiling Mounted PV system	(3) Microclimate
(4) Chair Fans	(5) Thermal Manikin	(6) Macroclimate

(b)

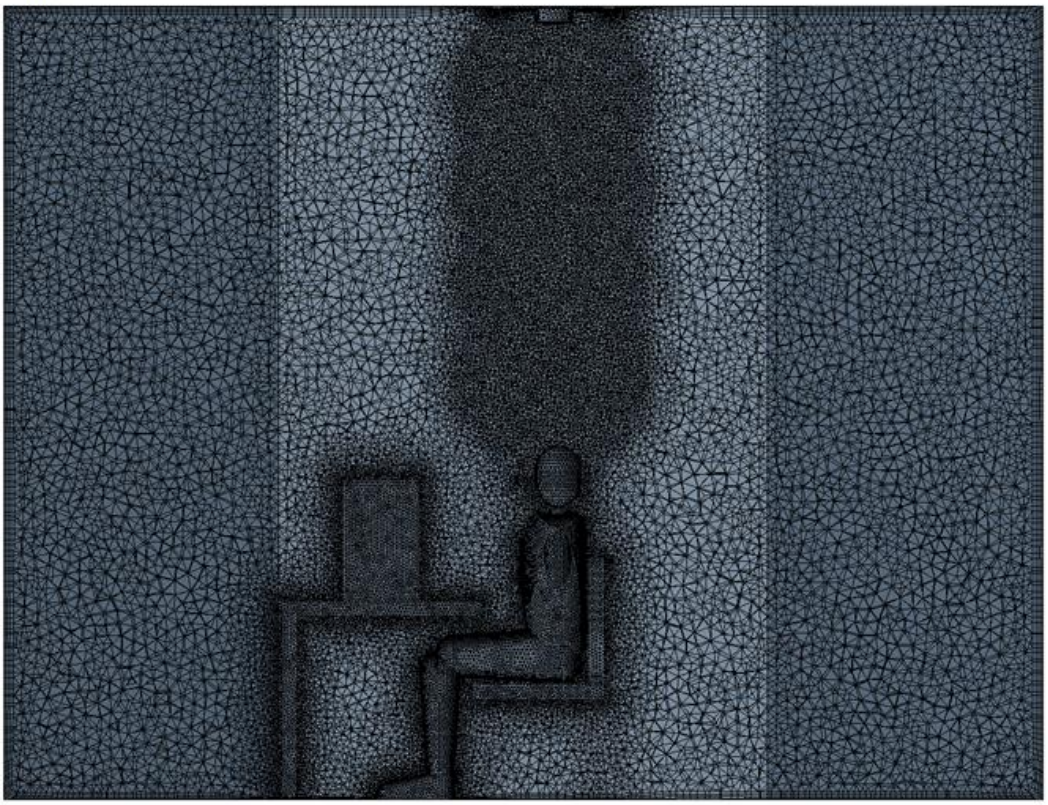

Figure 3 - (a) the computational domain used in the simulations (b) the generated grid

Moreover, a fine grid was developed near the surfaces to accurately capture the shear-layer entrainment, and to capture all the thermal plumes present in the space. A tetrahedral unstructured mesh (as shown in Fig. 3b) was generated using an element size of 2 cm on the surfaces. In addition, spheres of influence above the occupant were created to capture the velocity boundary layers and the rising plume. The air in the room is modeled as a continuous fluid hence it is appropriate to simulate using the Eulerian approach. There are plenty of different turbulence models available in ANSYS Fluent; each of them solves the Navier Stock equations by modeling them in a specific way. Some turbulence modeling methods are quite advanced (such as the large eddy simulation (LES)); however the computational cost of such methods is really expensive. One of the widely used turbulence models is the realizable k-ε turbulence which was also selected in addition to the enhanced wall treatment option. The realizable k-ε model correctly predicts the flow having round jets, circulations, and separation [17, 22]. The ideal gas law was used to model the density variation when it comes to account for buoyancy. The CFD software discretizes the Navier Stock equations; the discretization scheme selected for this work was the second order up wind to solve for the momentum, k, ε, and energy equations. The "PRESTO!" staggered scheme was used for the pressure

[22, 28]. For the velocity and pressure coupling the SIMPLE algorithm was selected and found most appropriate for this work. To have a proper CFD modeling, it is necessary to specify the right boundary conditions for the set up. For airflow modeling, the supply velocity that is normal to the outlet of the nozzle, the turbulence intensity and velocity were specified. The exhaust was modeled as a pressure outlet with zero gage pressure. For the chair fans, the "fan" boundary condition was imposed at the inlet of the chair fan at a specified pressure jump [17, 21]. Thermally, heat fluxes were imposed on the walls and the ceiling to mimic a real office internal load. Different occupant activities impose different metabolic rates, thus having an effect on the rising thermal plume, for this current work; in an office space the occupant is performing "light work". Carbon dioxide (CO_2) was used as tracer gas to assess for indoor air quality. The tracer gas was injected in the ceiling peripheral diffusers to simulate recirculated air; moreover a constant dose of CO_2 was injected to the room to mimic a typical CO_2 emission in an office. Furthermore, the under relaxation factors were carefully manipulated to dampen the scaled residuals to speed up convergence. Table 1 summarizes all the boundary conditions and schemes used in the simulation for the case studies.

Table 1- Boundary Conditions and Schemes used in the Simulations

Parameter/Model	**Properties**
Turbulence Model	Realizable k-ε model
Numerical Schemes	Second Order Upwind ; SIMPLE algorithm; PRESTO scheme for Pressure
Ceiling	Constant Light Load of $10W/m^2$
Floor, Desk, Chair	Adiabatic wall
Human Body (Manikin)	Constant Skin Temperature of 11 body segments from the coupled calculations
Computer	Constant heat flux resulting in total heat 93 W
PV nozzle	Velocity Inlet of 17 cfm (8.5 L/s) of Fresh air (400 ppm of CO_2), Turbulence Intensity 2.5%, and Turbulence Length scale 0.0006m
Peripheral Diffusers	Angled at 45°, Total flow rate of 50 L/s (recirculated air) , Turbulence Intensity 2.5 %, and Turbulence Length scale of 0.006 m
Exhaust	Pressure Outlet
Chair Fans	Fan boundary layer with specific pressure depending on the flow rate
CO_2 Source	Velocity inlet Turbulence Intensity 7.7%, Hydraulic Diameter 6 mm

To set up the CFD model that can predict the real physics of such complex air flow interactions the momentum method was selected [17]. It is important to mesh the computational domain properly because one is interested in capturing the true physics of the problem, while maintaining the minimum computational cost. Inflation layers were added in three places to capture the boundary layer at the manikin, nozzle, ceiling, and walls of the room. The inflation layer that was created around the manikin was a first layer thickness of 1.8 mm, at a growth rate 1.1, and a total number of three layers. Buoyancy effects were taken into account by using the incompressible ideal gas law. The dimensionless wall distance y^+ that is defined by the following equation:

$$y^+ = \frac{u^* y}{\nu} \qquad (1)$$

where u* is the friction velocity, y is the distance to the nearest wall, and ν is the kinematic viscosity. In regions where y^+ is of order of unity, the two layer model is used and the laminar sub-layer is resolved. However, when y^+ ranges between 3 and 10, an enhanced wall treatment is used. Consequently, the y^+ value ranged between 0.9 and 4.5 on the surface of the manikin.

The jet that is coming out of the nozzle is being entrained by contaminated surrounding air. To capture this entrainment, four spheres of influence of 1 m diameter were integrated in the meshing of the microclimate. The grid in this specific region is

compacted and clustered, and the element size was chosen to be 2 cm. Finally a grid independence test was performed to choose the appropriate grid for simulation, where the results are independent of the number of elements. Two parameters were monitored: the macroclimate temperature and the CO_2 concentration at the breathing zone. The results of the tested grids are presented in Table 2.

Table 2- The grids used for mesh independency

Grid Type	Face Size Element (cm)	Number of Elements	Maximum Relative Error in predicting the values of Macroclimatic Temperature and CO_2 concentration when compared to the previous mesh values
Coarse	3	707,520	-
Medium	2.5	1,415,040	15.3%
Fine	2	2,830,080	5.5%
Very Fine	1.5	5,660,160	4.4%

The described mesh treatment resulted in a total number of elements equal to 2,830,080 elements for the entire computational domain as shown in Fig. 3b. Numerical convergence was judged using mainly three criteria: (1) scaled residuals reported by Fluent should reach a minimum of the order 10^{-5}; however convergence was not reached

until (2) the net heat flux of the computational domain was below 1% of the total heat gain and (3) the CO_2 concentration at the breathing zone stabilized.

3.1.2 Air quality modeling

In this work, air is modeled as a continuous fluid and the Eulerian approach is adopted. To investigate the level of mixing between the supplied air and the stagnant air in the room (contaminated air), the ventilation effectiveness is assessed using a tracer gas, which in this study is carbon dioxide gas. The fresh air nozzle in the ceiling has a CO_2 concentration of a mean value of 400 ± 50 ppm, a typical value of outdoor CO_2 concentration. It is important to note that the amount of fresh air coming in to the room is equal to the amount of air leaving the room through the exhaust; this way no CO_2 accumulation will remain in the room. A typical CO_2 emission (0.31 L/min/person) [30] is used in an office space.

Ventilation effectiveness is defined as ε_v:

$$\varepsilon_v = \frac{C_R - C_B}{C_R - C_F} \qquad (2)$$

where C_R is the CO_2 concentration of the return or recirculated air, C_B is the CO_2 concentration at the breathing zone of the manikin, and C_F is the CO_2 concentration in the fresh air supplied to the workspace. Typically all concentrations are measured in

ppm. The CO_2 concentration of the air supplied by the primary nozzle is in the range of 300-500 ppm according to the ANSI/ASHRAE Standard 62.1-2013 [30, 31]. The equation above refers to the air quality index (AQI) at the breathing zone of the manikin. The breathing zone is defined to be a sphere of radius 1 cm located at a distance of 2.5 cm from the nose of the manikin. The near head temperature and velocity are defined to be at a distance of 5 cm offset from the head of the occupant.

The species transport model is enabled to help calculating the carbon dioxide concentration field, thus assessing the indoor air quality. Moreover, the turbulent Schmidt number is defined by being proportional to the ratio of viscous diffusion rate over the mass diffusion rate. The dimensionless Schmidt number is given by the following equation:

$$Sc = \frac{\mu_t}{\rho D_t} \tag{3}$$

where μ_t is the turbulent viscosity of air, ρ is the density of species i.e. in this case CO_2, and D_t the turbulent diffusion rate of carbon dioxide. In previous studies in literature about gas reactions, Sorensen et al. reported that when the value of the dimensionless Schmidt number is bounded between 0.9 and 1, this shows a better agreement with the experimental results. Therefore a value of 0.95 will be adopted [16, 17].

3.1.3 Bio Heat Model

The CFD model is coupled with a validated bioheat model to calculate the skin temperature of the thermal manikin at each segment of its body. The model is coupled with Zhang's thermal comfort models mainly to assess the local comfort based on the resulting segmental temperature. The bioheat model divides the thermal manikin into eleven segments. The segmental parts are as following: head, chest, abdomen, back, buttocks, claves, thighs, upper arms, lower arms, hands, and feet. The physiological response is simulated at each segment to predict the thermal comfort based on Zhang's model of comfort [25-27]. This coupling phase of the simulation will help in capturing the effect of the flow and the natural human response under specific circumstances. The integration of the CFD model with that of the bioheat model is demonstrated in Fig. 4. At first, the skin temperature is chosen to be that of a typical human being skin temperature in a "thermo-neutral" condition, then the CFD simulation runs until convergence is reached. From ANSYS, the air temperature at the vicinity of segmental body parts and the segmental heat transfer coefficient are obtained. These two parameters are used as inputs to the bioheat model which will result in the updated segmental skin temperature. This iterative procedure is repeated until convergence is achieved. The criterion of convergence is when the segmental skin temperatures of two consecutive iterations differ by less than 10^{-3}.

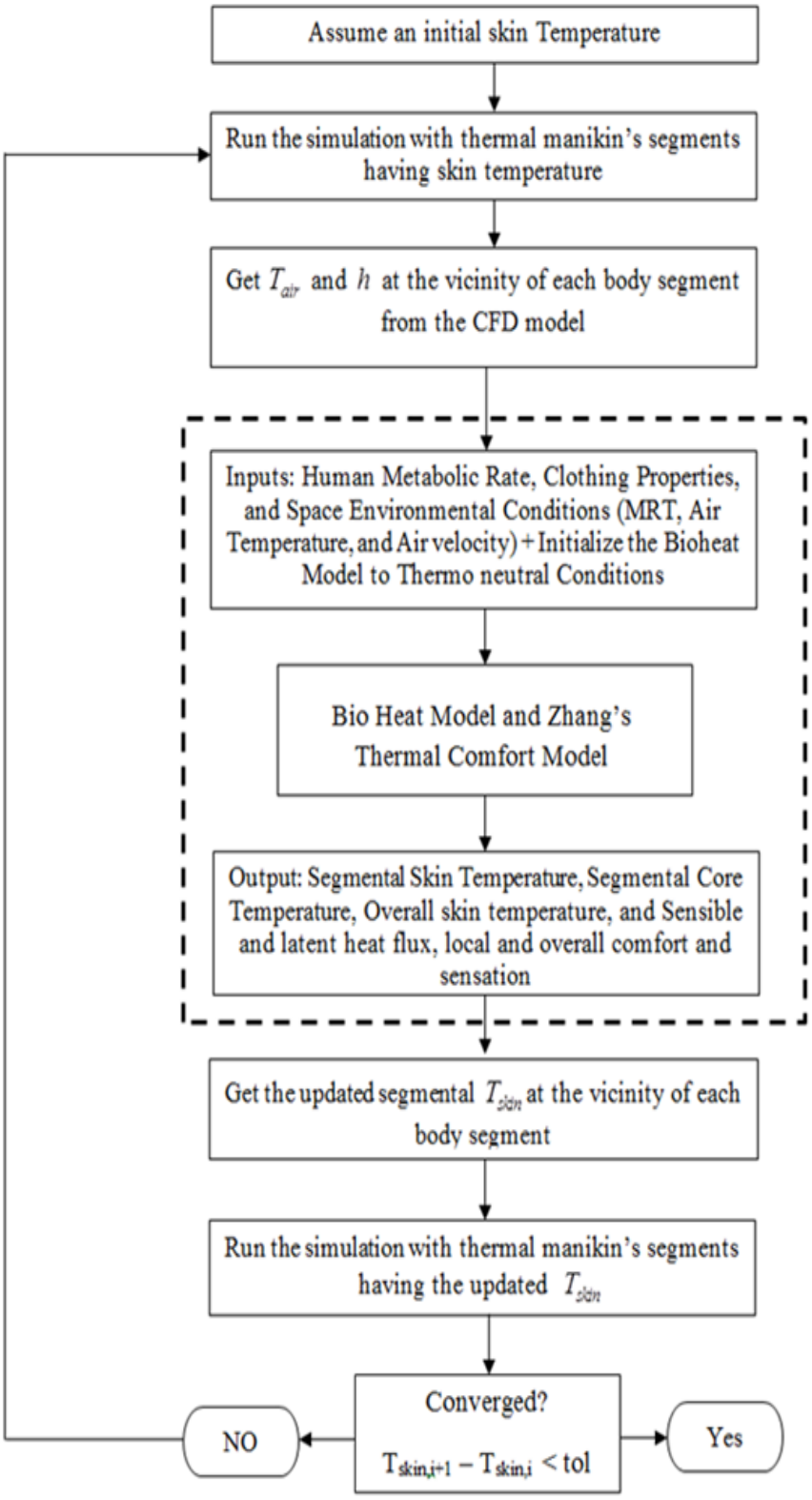
Assume an initial skin Temperature
Run the simulation with thermal manikin's segments having skin temperature
Get T_{air} and h at the vicinity of each body segment from the CFD model
Inputs: Human Metabolic Rate, Clothing Properties, and Space Environmental Conditions (MRT, Air Temperature, and Air velocity) + Initialize the Bioheat Model to Thermo neutral Conditions
Bio Heat Model and Zhang's Thermal Comfort Model
Output: Segmental Skin Temperature, Segmental Core Temperature, Overall skin temperature, and Sensible and latent heat flux, local and overall comfort and sensation
Get the updated segmental T_{skn} at the vicinity of each body segment
Run the simulation with thermal manikin's segments having the updated T_{skn}
Converged?
$T_{skin,i+1} - T_{skin,i} < tol$
NO
Yes

Figure 4- Flow chart showing the algorithm for coupling between CFD and bioheat model

3.2 Experimental Protocol

The experimental setup was constructed in a controlled climatic chamber ventilated by a ceiling mounted personalized ventilation system. Primarily, the experiment aimed to validate the CFD model in terms of indoor air quality and thermal comfort. The validation consisted of comparing the measured and predicted segmental skin temperatures, velocity and temperature near head of the occupant, and ventilation effectiveness.

The climatic chamber (3.4 m × 3.4 m × 2.8 m) that was used to validate the numerical model is constructed of highly insulated ceiling and floor and has an internal layout of a typical office. The air distribution system consists of a single nozzle 9 cm in diameter that supplies fresh air, and four peripheral diffusers that supply recirculated air at an angle of 45°. This angled diffuser flow will aid in creating a canopy effect around the occupant, thus aiding in the localization of the flow. The fans have a single degree of freedom mechanism in which they are allowed to move up-and-down vertically.

Beneath the ceiling mounted personalized ventilation system, a thermal manikin is used to report all the measured data. The thermal manikin “Newton”, manufactured by Northwestern Measured Technology [33], is divided in twenty independently controlled zones, where each reports segmental comfort, sensation, skin temperature,

and generated heat flux. The thermal manikin has its own software whereby it is being coupled to maintain a constant core temperature while skin temperature and heat flux generated vary with different conditions. Prior to every experiment, the manikin must be initialized to a typical human body in neutral conditions. The thermal manikin was dressed with a typical office outfit which is a long sleeved shirt, and pants. The clothes worn by the manikin have an overall resistance of 0.6 clo, which is the typical clothing resistance in an office for a man. “Newton”, shown in Fig. 5a, is best used to detect any change in the environmental conditions, consequently mimics a human’s physiological response such to any change in the surrounding.

Figure 5- (a) the thermal manikin that was used in the experiment (b) the chair fan mechanism

The ceiling mounted nozzle integrated with a slot diffuser is placed at the middle of the room, right above the manikin's head. On the manikin's chair, four fans are mounted two on each side. In the room, two symmetrically exhausts are installed. A desktop computer generating 93 W [17] was placed on the desk in front of the manikin, as represented in Fig. 1. The return duct was seeded with 0.0035 L/s [17] flow rate of carbon dioxide to represent return air. A constant CO_2 dose of 0.31 L/min/occupant was used in the experiment to mimic a typical CO_2 office load that was emitted from

equipment, furniture, and occupants [30]. The tracer gas was injected into the room through a tube; the tubing was optimized for uniformity of tracer gas distribution [4, 9]. The thermal plume generated by the thermal manikin produced nearly 75 W, in addition to the lighting load that was almost 10 W/m^2. The air conditioning of the space was via two Honeywell (2.64 kW) air handling units. One of the air handling units supplies fresh air to the *PV* nozzle, while the other AHU supplies return air to the peripheral diffusers. The experimental setup allows variation in fans' height and flow rate. The fan mechanism, shown in Fig. 5b, allowed variation of the height ranging between 30 cm to 50 cm above the ground. On the other hand, the flow rate of the fan is controlled by a 12 V DC-dimmer. The total flow rate of the fans can vary between 5 L/s to 15 L/s.

To reduce the turbulence intensity and air flow mixing the primary nozzle was fitted with honeycomb flow straighteners resulting in a thickness over diameter ration $t/d = 7.5$ which lies in the recommended range for optimal results [35]. Moreover, velocity and turbulence measurements at the outlet of the *PV* nozzle were measured using a TSI manufactured omni-directional hotwire anemometer having an accuracy of $\pm$ 3%. The hotwire anemometer was pre-calibrated for low velocities ranging less than 2 m/s.

On the other hand, air quality was assessed by taking CO_2 samples that were obtained by measuring the CO_2 concentration using FIGARO CDM4161- CO_2 sensors

having an accuracy having ± 20 ppm. Six CO_2 sensors were installed in the following configuration, two sensors were place at breathing zone of the occupant, two other sensors were placed at the return air inlet, and the final two sensors were placed at the nozzle outlet to measure the CO_2 concentration in the fresh air supplied to the room. At steady state conditions, the effectiveness of each experiment was computed to compare it with that predicted by CFD model.

For thermal and flow field assessment, measuring the segmental skin temperature and the temperature and velocity near the head of the manikin are mandatory to obtain a valid model. A set of 11 K-type thermocouples having an accuracy of ± 0.5 °C manufactured by Omega were distributed around the body parts of the thermal manikin as shown in Fig. 6. The thermocouples are connected to OMEGA DaqPro data logger to store the data.

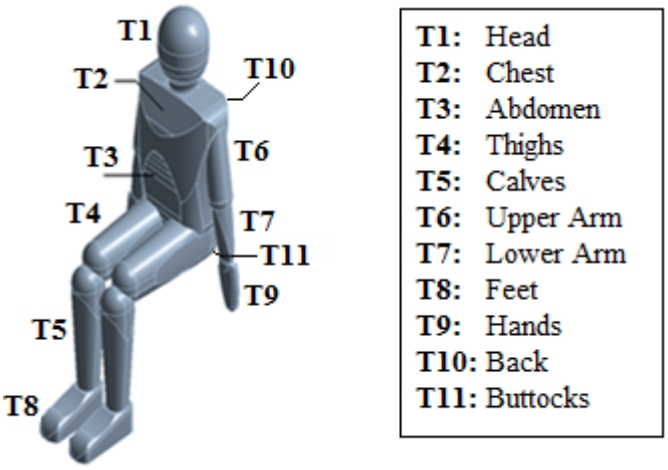

Figure 6 - Thermocouples distributed over the segmental parts of the thermal manikin, the thermal manikin‘s representation is a default dummy in the commercial CFD software ANSYS

Table 3- The conducted experiments used for model validation

Experiment Number	Fan Mode	Fan Height (cm)	Total Fan Flow Rate (L/s)
1	OFF	-	-
2	ON	30	10
3	ON	40	10
4	ON	50	15

For model validation, four experiments were conducted, as tabulated in Table 3. Makhoul et al. [17] have shown that having a fresh air flow rate of 15 cfm (7.5 L/s) and a temperature of 16 °C results in a good thermal comfort and indoor air quality specifically with the use of fans. In addition, the temperature and flow rate (16 °C and 50 L/s) of the peripheral diffusers were also kept constant. The peripheral diffusers delivered return air at an angle of 45° to obtain optimal localized flow around the occupant [15-17]. To ensure steady state conditions, the experiments lasted at least three hours, and the data was recorded when the readings of CO_2 concentration, temperature fields, and velocity stabilized.

3.3 Parametric Study

After validating the model through experimentation, the validated CFD model was used to a typical office case (3.4 m × 3.4 m × 2.6 m), where the effectiveness of the chair fans in terms of comfort and indoor air quality is investigated. Moreover, the parametric study served also to help in finding optimal combination of fan flow rate and height that result in best ventilation effectiveness and thermal comfort. In the parametric study, the total load in the space is kept similar to a typical load in an office that is equal to 60 W/m^2. The fresh flow rate was set to the newly updated ASHRAE recommendation of 17 cfm (8.5 L/s) [31, 34]. The temperature of the fresh air and the

recirculated air supplied by the peripheral diffusers was set to be 16 °C. For each simulation, the room was divided into two zones: macroclimate and microclimate. The validated bioheat model was used to couple the CFD model in order to mimic a human response to the available environmental conditions. For the purpose of finding an optimal height and flow rate, three sets of simulation cases are conducted. Table 4 presents all the simulation cases that were conducted to find the optimal height and flow rate to attain the best combination of thermal comfort and indoor air quality.

Table 4- Simulation Cases used in the parametric study

Simulation Cases	Fan Height (cm)	Total Fan Flow Rate (L/s)
Set 1	30	5
		7.5
		10
		12.5
		15
Set 2	40	5
		7.5
		10

		12.5
		15
Set 3	50	5
		7.5
		10
		12.5
		15

CHAPTER IV

RESULTS AND DISCUSSION

The localized HVAC system was studied to obtain the optimal height and flow rate of the fan. The aim of this part is to find the best (optimal) combination of fan height and flow rate to attain best IAQ and thermal comfort at minimum energy cost. This is achieved by comparing the performance of the chair fans at three different levels and at five different flow rates as tabulated in Table 4. The performance of each case was assessed by observing the achieved air quality, the perceived thermal comfort. After figuring out the optimal height and fan flow rate, the optimized system is then compared to the conventional mixing ventilation system to check its energy savings. It is important to note that all other parameters that might affect the thermal comfort and IAQ are kept constant, such as the fresh air flow rate which is fixed at 17 cfm (8.5 L/s) as recommended by ASHRAE standard 62.1 – 2013 [28] and having a temperature of 16 °C. The peripheral diffusers had a total flow rate of 50 L/s [15-17] and temperature of 16 °C. The bioheat model is coupled with the CFD model to generate the human response to the varying external conditions. Then, Zhang's comfort models [23-25] are used to calculate the segmental and overall comfort and sensation.

4.1 CFD validation

Since the CFD model was coupled with the bioheat model, it was necessary to validate the predicted results to ensure that the coupling process was able to capture the human-response to the localized environment in a *PV* + CF system. To validate the CFD model, the segmental skin temperature, the near head temperature and velocity, and the ventilation effectiveness were measured experimentally and compared to those predicted by the numerical model. It was important to validate the flow field from the *PV* jet due to use of the momentum method that was selected to model the diffuser's jet. Four experiments were conducted at different fan elevations at 30 cm, 40 cm, and 50 cm in addition to having chair fans turned OFF (see Table 3).

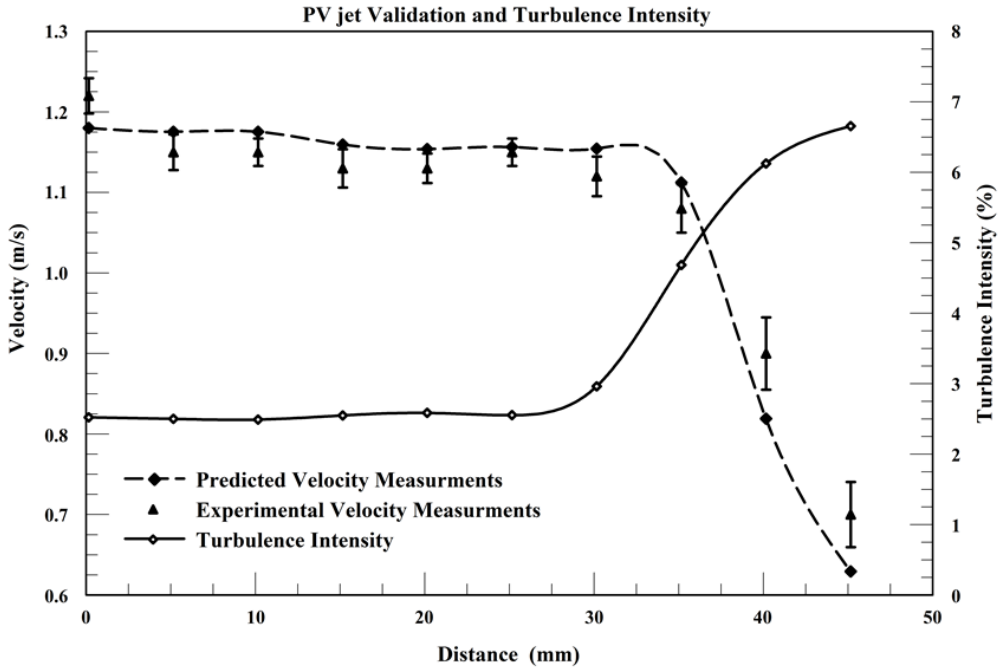

Figure 7- PV nozzle jet validation and turbulence intensity as function of distance away from the nozzle

Figure 7 shows the plot of experimental velocity measurements and those predicted by the CFD for the *PV* nozzle flow. In addition, the turbulence intensity is plotted at different position of the flow, a value of 2.5% was selected as boundary condition in the for the *PV* nozzle. Figure 7 shows good agreement between the measured velocities and those predicted by CFD model having a maximum relative error of 10.1%. The measurements of the velocities were taken at 5 mm increment distances starting from the nozzle of the *PV* until a distance of 45 mm (vertically) is reached.

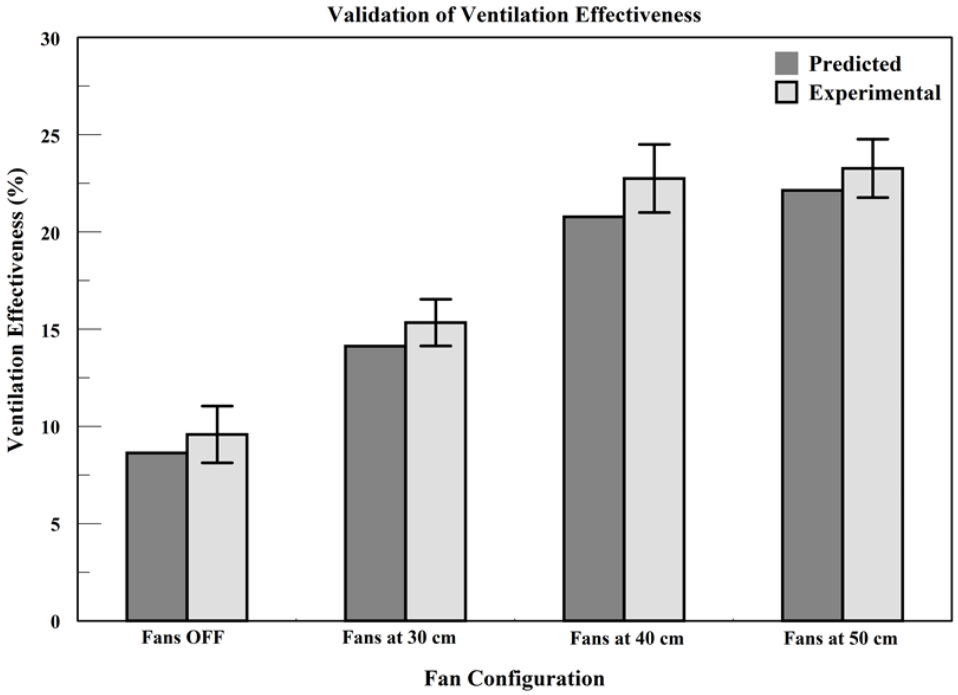

Figure 8- The measured and the predicted ventilation effectiveness at the breathing zone for a single PV system having fresh flow rate of 7.5 L/s and T = 16 deg C and total fan flow rate of 10 L/s

Moreover, the predicted segmental skin temperatures were compared to those measured experimentally. All four experiments reported good agreement between the predicted segmental skin temperatures and the measured values. Figure 9(a-d) shows the results of measured segmental skin temperature on the thermal manikin and those predicted by the CFD model for all fan configurations a) Fan OFF, (b) 30 cm, (c) 40

cm, and (d) 50 cm (see Table 3). It is noticed that the numerical model was able to predict accurately the segmental skin temperature of the occupant since the relative error obtained was less than 4%. Figure 9(a-c) show clearly the segmental skin temperature decreases as the height of the fan increases. For instance, the skin temperature measured on the head dropped by 0.67 °C when comparing between fan levels 30 cm and 50 cm.

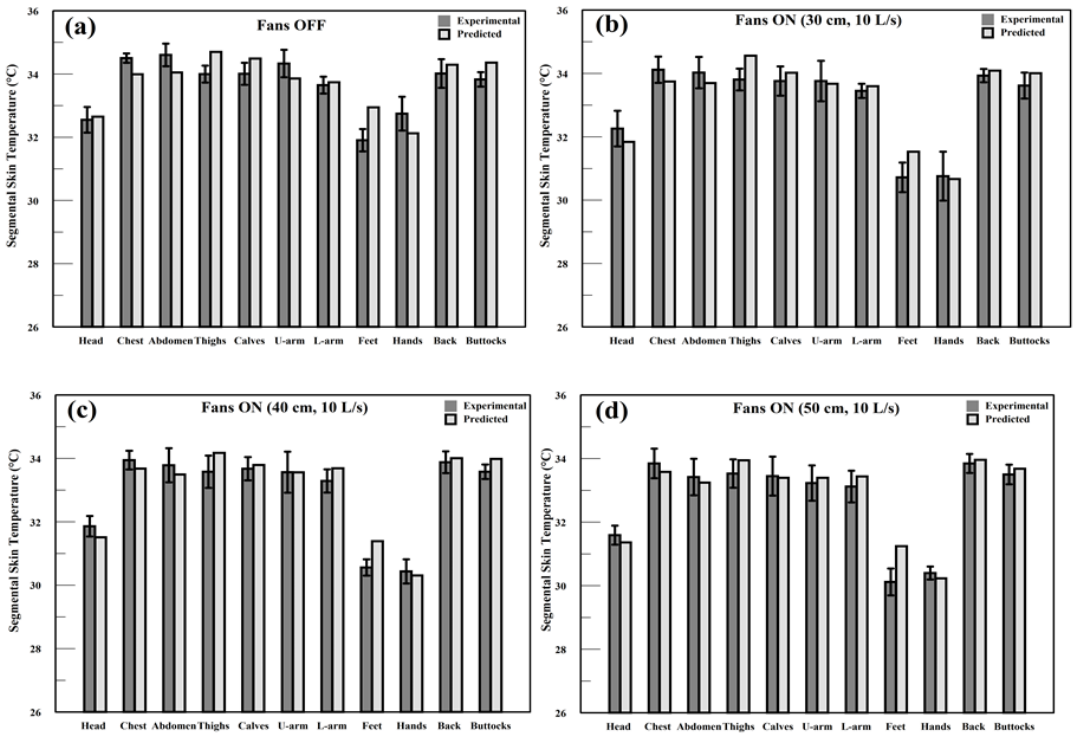

Figure 9- Segmental Skin validation: (a) Fans OFF (b) Fan H=30 cm (c) Fan H=40cm (d) Fan H=50 cm; at Q = 10 L/s

Table 5- Model Validation: The near head velocity and temperature of the measured values versus predicted values by CFD model for case of PV jet of 7.5 L/s and temperature of 16°C

Fan : Elevation	Measured Near head Temperature (°C) Accuracy (±0.50 °C)	Predicted Near head Temperature (°C)	Measured Near head Velocity (m/s) Accuracy (± 3%)	Predicted Near head Velocity (m/s)
OFF	25.73	25.85	0.37	0.35
ON : 30 cm	25.41	25.56	0.42	0.44
ON : 40 cm	24.96	24.92	0.47	0.49
ON : 50 cm	24.60	24.51	0.56	0.59

In addition, Table 5 presents the near head temperature and velocity as compared to the values predicted by the CFD model. The numerical model was able to capture the physics of the flow and thermal interaction between the plume and the PV jet and induced fan flow as indicated by the good agreement between the measured values and the predicted ones. The relative error varied from 4% up to 6% for the near head velocity measurements, whereas for the near head temperature the error remained in the ± 0.5 °C range (i.e. the instrumental error due to the thermocouple) for different fan levels.

The air quality was assessed using the ventilation effectiveness ε_v, and the results are plotted in Fig. 8 for three different fan heights (of 30 cm, 40 cm, and 50cm) running at constant total fan flow rate of 10 L/s. Figure 8 shows good agreement between the values obtained by the CFD model and those of the experiment with relative error varying from 4.80 up to 9.90 % for different fan heights. From the data obtained, it is clear that the AQI (ε_v) increases with increasing fan height while maintaining a constant fan flow rate since the ventilation effectiveness was 22.14 % at 50 cm compared to an effectiveness of fans OFF (8.62%). The predicted ventilation effectiveness values were compared to the experimentally measured values the CO_2 sensors described in the experimental protocol. The results were in good agreement with the CFD data, since the *PV* is supplying 7.5 L/s, and this is relatively a high flow rate.

4.2 Parametric Study

The aim of this part is to find the best (optimal) combination of fan height and flow rate to attain best IAQ and thermal comfort at minimum energy cost. This is achieved by comparing the performance of the chair fans (in terms of thermal comfort and IAQ) by varying the height of chair fans and their flow rates (see Table 4).

4.2.1 Air quality comparison

In this section, the effect of fan height and flow rate on ventilation effectiveness is studied. The low temperature of the supplied *PV* jet has a positive effect on the air quality of the inhaled air due to the buoyancy forces generated by the cold jet that will be acting downwards. Table 6 lists the ventilation effectiveness at three different heights having various fan flow rates ranging from 5 L/s to 15 L/s. It is clear that as the fan level increases while maintaining relatively low fan flow rates (ranging from 5 L/s up to 10L/s), ventilation effectiveness increases remarkably. For instance, at a total fan flow rate of 7.5 L/s the reported ventilation effectiveness was 12.47%, 16.77%, and 19.72% at fan height of 30 cm, 40 cm, and 50 cm respectively. However when fan flow rates exceed 10 L/s a counter effect on the ventilation effectiveness is observed due to mixing effect of recirculated air. For instance, this is illustrated by comparing between the effectiveness at a total fan flow rate of 10 L/s and 15 L/s at every fan height (30 cm, 40 cm, and 50 cm). The reported ventilation effectiveness dropped by 3.22%, 4.30%, and 7.45% at 30 cm, 40 cm, and 50 cm respectively. It is important to note that the mixing effect is dominant at high fan levels due to the fact that at relatively high fan level, the thermal plumes generated by the occupant (at trunk level of the body) tend to be stronger (i.e. having higher velocities). This will generate a recirculated flow from the contaminated region to the microclimate region of the occupant driven by the plumes'

higher upward velocity. Therefore, the fans' high flow rate will aid in increasing the mixing effect. Nonetheless, it is important to note that despite this "mixing" effect, the ventilation effectiveness that was reported at fan level of 50 cm and total fan flow rate of 15 L/s (18.16%) is almost double that when compared to the same case when chair fans are turned OFF (9.31%). On the other hand, when fixing the height of the fans, the ventilation effectiveness keeps on increasing until reaching a peak at total flow rate of 10 L/s as shown in Fig. 10(a-c), whereby after that i.e. at higher fan flow rates the effectiveness drops again due to the mixing effect. However, the peak of ventilation effectiveness increase as the fan level increases, having a maximum of 23.39% at high levels (50 cm) and a minimum of 13.67% at low levels (30 cm). At high levels, high effectiveness is achieved due to ability of the chair fans to suck the rising plumes effectively and pulling more fresh air to the breathing zone of the occupant. Consequently, the maximum ventilation effectiveness is achieved at height of 50 cm and total fan flow rate of 10 L/s.

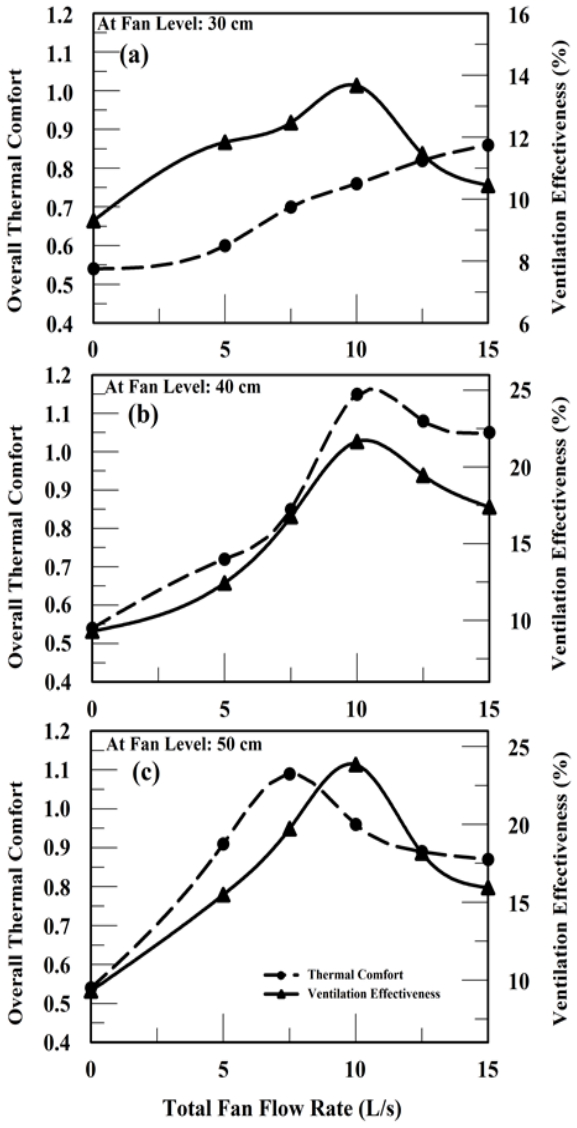

Figure 10 - Overall comfort and Ventilation effectiveness as function of total fan flow rate at fan level (a) 30 cm (b) 40 cm (c) 50 cm

4.2.2 Thermal Comfort

Thermal comfort of the occupant is directly affected by the height and flow rate of the chair mounted fans. Figure 11 (a-b) shows the overall (a) thermal comfort and (b) thermal sensation perceived by the occupant when varying fan heights and flow rates.

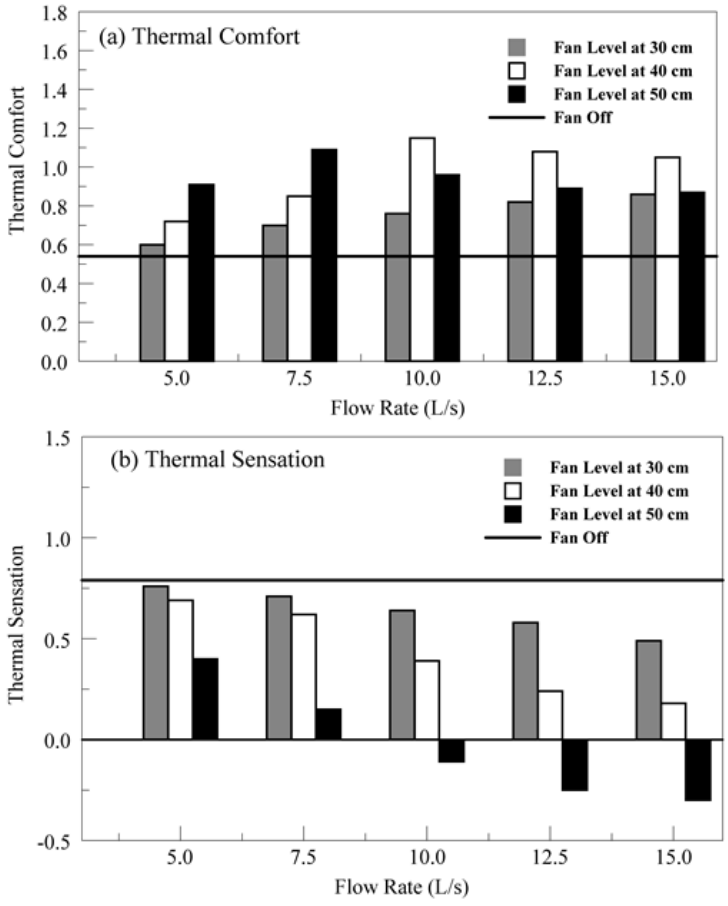

Figure 11- overall (a) comfort and (b) sensation for different fan configuration

When comparing the effect of the chair mounted fans on the induced thermal comfort, a net enhancement is attained when the chair fans are turned ON. It is noticed that as the fan level increases while maintaining low fan flow rates (ranging from 5 L/s up to 7.5 L/s), thermal comfort also increases. For instance, at a total fan flow rate of 7.5 L/s the perceived thermal comfort reported at fan level of 30 cm, 40 cm, and 50 cm were 0.70, 0.85, and 1.09 respectively. However, this is not the case when the total fan flow rate exceeds 7.5 L/s. Conversely at total fan flow rate of 10 L/s the perceived thermal comfort was 0.76, 1.15, and 0.96 at fan height of 30 cm, 40 cm, and 50 cm respectively. It is noticed that at high fan level (50 cm) and high fan flow rate (exceeding 7.5 L/s) the thermal comfort decreases, this is mainly due to the thermal draft caused by the cold sensation at the head.

Table 6- Comparison of the ventilation effectiveness, near head velocity, and near head temperature having chair fans fixed at height of 30 cm, 40 cm, and 50 cm at different fan flow rates, PV jet having 8.5 L/s

Total Fan Flow Rate (L/s)	Fans at Level of 30 cm			Fans at Level of 40 cm			Fans at Level of 50 cm		
	Near head Temp. (°C)	Near head Velocity (m/s)	ε_v	Near head Temp. (°C)	Near head Velocity (m/s)	ε_v	Near head Temp. (°C)	Near head Velocity (m/s)	ε_v
5	25.56	0.39	11.84	25.11	0.42	12.45	24.65	0.52	15.49
7.5	25.50	0.42	12.47	25.02	0.46	16.77	24.54	0.55	19.72
10	25.44	0.45	13.67	24.87	0.50	21.69	24.43	0.59	23.39
12.5	25.39	0.47	11.46	24.74	0.53	19.46	24.37	0.61	18.16
15	25.27	0.49	10.45	24.66	0.56	17.39	24.19	0.64	15.94

However, at fixed fan height, three phenomena were observed. At high fan levels, the fans will successfully pull down more fresh air, however having higher velocity and lower temperature. Therefore at high fan level (50 cm) and high fan flow rate (exceeding 7.5 L/s) the thermal comfort decreases, this is mainly due to the thermal draft caused by the cold sensation at the head. One the other hand, at fan level of 40 cm,

it is observed that at a total fan flow rate of 10 L/s the thermal comfort peaks attaining a value of 1.15. On the other hand, at low levels (30 cm), the thermal comfort keeps on increasing up to 0.86 (at total fan flow rate of 15 L/s) due to the absence of any thermal draft on the head. Therefore, the maximum thermal comfort perceived by the occupant was reported to be 1.15 attained at fan height of 40 cm and total fan flow rate of 10 L/s.

It is critical to monitor the near head temperature and near head velocity to check for any thermal draft. If velocity exceeds 0.4 m/s [39] at relatively low temperatures, cold sensation will cause thermal draft having a PD (Percentage Dissatisfaction) of less than 10%. Table 6 indicates that by increasing the height at which the fans are fixed on, the ventilation effectiveness increase, near head temperature decreases, and near head velocity increases. It is clear that at high fan heights (at 50 cm above ground level); higher velocities (up to 0.64 m/s) and lower temperatures (24.19 °C) are reached.

To analyze the perceived thermal comfort in detail, it is important to observe the segmental sensation and comfort, especially at the critical location which is the head. Table 7 presents the segmental thermal comfort and sensation, as predicted by the bioheat and comfort models, under a selected fan height of 40 cm. Clearly, the most affected body segments by the performance of the chair fans are located in the upper body specifically the head, chest, abdomen, and the back. The head is the most highly affected since it is first hit by the fresh air *PV* jet, before spreading over the rest of the

body. As the chair fans are turned on, an improvement of segmental thermal comfort along with a slight decrease of the thermal sensation is noticed since the affected body segments are exposed to cooler air at higher velocities. The rest of the body parts i.e. the lower parts are affected in a minor manner since they are exposed to nearly the same climatic conditions. It is logical that the lower body parts are least affected by the system, since as presented in Table 7, the segmental comfort of the lower body parts show low or negligible change in comfort. Previous studies have shown that lower body parts are slightly sensitive for any cooling needs [36]. Additionally, since the macroclimate temperature is maintained at relatively higher temperatures (26 °C) therefore the probability of having any thermal drafts sensation because of the *PV* jet is minimum [37, 38]. Therefore, the impact of the air movement created by the suction chair fans can be neglected [17]. Figure 12 (a-c) displays the contour plots of (a) velocity, (b) temperature, (c) CO_2 concentration fields at a selected case having fan height of 40 cm and a total fan flow rate of 10 L/s.

Fan Flow Rate (L/s)	Parameter	Head	Chest	Back	Abdomen	Buttocks	Upper Arm	Lower Arm	Hands	Thighs	Calves	Feet	Overall
0	Comfort	1.32	1.45	-0.34	0.58	0.53	125	0.25	0.63	1.12	0.61	1.69	0.54
	Sensation	-0.39	1.24	1.37	0.49	0.31	0.90	1.51	0.62	0.59	0.72	0.74	0.79
5	Comfort	1.35	1.45	-0.26	0.73	0.69	1.34	0.63	0.72	1.40	0.92	1.69	0.69
	Sensation	-0.43	1.20	1.34	0.40	0.23	0.84	1.30	0.59	0.39	0.41	0.72	0.72
7.5	Comfort	1.37	1.43	-0.08	0.88	0.79	1.45	1.27	0.75	1.86	1.10	1.65	0.85
	Sensation	-0.44	1.16	1.25	0.32	0.21	0.77	0.94	0.61	0.08	0.26	0.70	0.62
10	Comfort	1.39	1.45	0.70	1.07	0.96	1.50	1.96	0.77	1.93	1.28	1.66	1.15
	Sensation	-0.64	1.03	0.78	0.26	0.23	0.74	0.58	0.67	-0.03	-0.02	0.66	0.39
12.5	Comfort	1.34	1.36	0.76	0.92	0.99	1.33	1.84	0.62	1.76	1.36	1.67	1.08
	Sensation	-0.87	0.98	0.81	0.43	0.31	0.84	0.68	0.82	-0.14	-0.21	0.38	0.24
15	Comfort	1.29	1.45	0.81	0.87	1.18	1.31	1.66	0.56	1.77	1.32	1.66	1.05
	Sensation	-1.00	0.85	0.82	0.48	0.20	0.86	0.78	0.88	-0.16	-0.18	0.32	0.18

Table 7- Segmental thermal comfort and Sensation for the selected cases at fan height of 40 cm

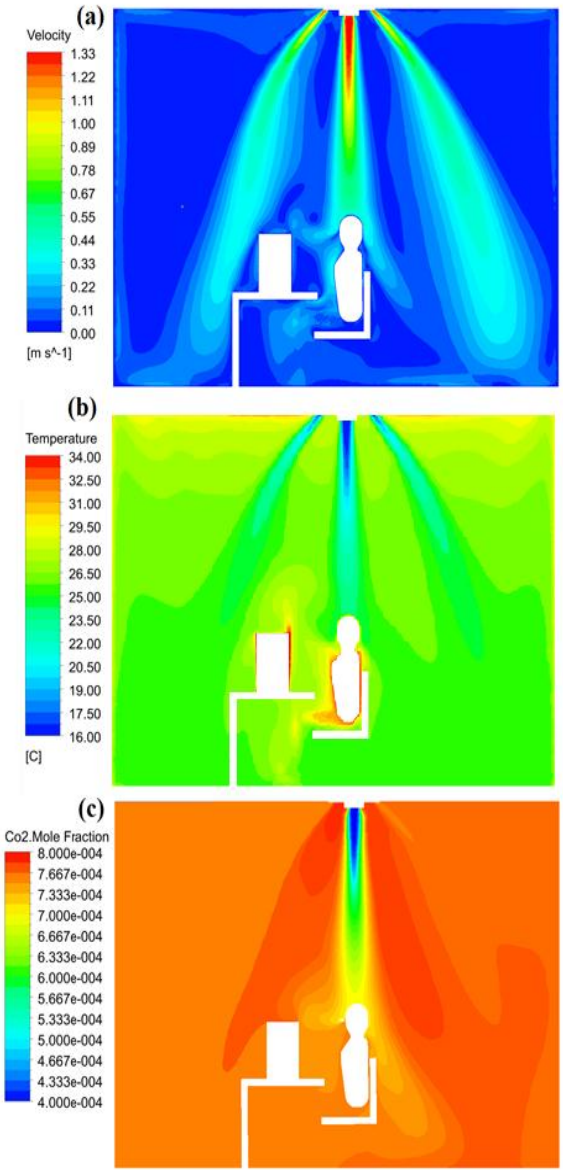

Figure 12- (a-c) displays the contour plots of (a) velocity, (b) temperature, (c) CO2 concentration fields at a selected case having fan height of 40 cm and a total fan flow rate of 10 L/s.

4.2.3 Energy Analysis

There are mainly two advantages of the novel system. The first advantage is that the proposed localized HVAC system provides high ventilation effectiveness with lower amount of fresh air supply. The second advantage is that the enhanced optimized system, allows having higher macroclimate temperature while maintaining acceptable thermal comfort due to the formation of the canopy around the occupant. These two properties of the enhanced proposed system entail a high potential in energy savings when compared to the conventional mixing ventilation, where a fraction of fresh air is mixed with the return air before being supplied to the room through the ceiling diffuser.

In order to calculate the energy savings associated with the option of assisting the ceiling mounted *PV* system with chair fans, an energy analysis was performed to estimate the cooling load for three selected cases: (1) Fan level 50 cm, at a total fan flow rate of 10 L/s (Highest attained IAQ), (2) Fan level 40 cm, at a total fan flow rate of 10 L/s (Highest perceived thermal comfort), and (3) the optimal case in terms of IAQ and thermal comfort. The calculations were based on equal thermal sensation for each simulated case separately so that the occupant will eventually have nearly the same comfort and sensation in the mixing ventilation system and in the selected (*PV + CF*) system cases. At the same amount of air flow rate, the systems are compared with the

conventional mixing ventilation system, however in order to achieve the same indoor air quality the equivalent amount of fresh air was used in the calculations.

Case 3 is defined to be the optimal case for both thermal comfort and indoor air quality. Since the maximum attained IAQ occurs at different fan configuration than that for thermal comfort, it is important to find a height and flow rate where there is best compromise for comfort and effectiveness. In other words, it important to check at which height there exist the least drop in thermal comfort and the least drop in ventilation effectiveness with respect to their maximum values. Figure 13 shows the normalized shift in ventilation effectiveness and thermal comfort as function of fan height. The normalized effectiveness values are calculated by taking the difference between the local effectiveness and its maximum value divided by the maximum value attained. Additionally, the sum of the normalized shifts of both comfort and effectiveness is plotted, and it can be inferred from Fig. 13 that the minimum shift is achieved at fan height of 47cm. It is clear that the least shift of the total percent drop in both (effectiveness and comfort) was achieved at fan height of 47 cm, where the corresponding absolute thermal comfort and effectiveness were 1.07 and 23.19% respectively.

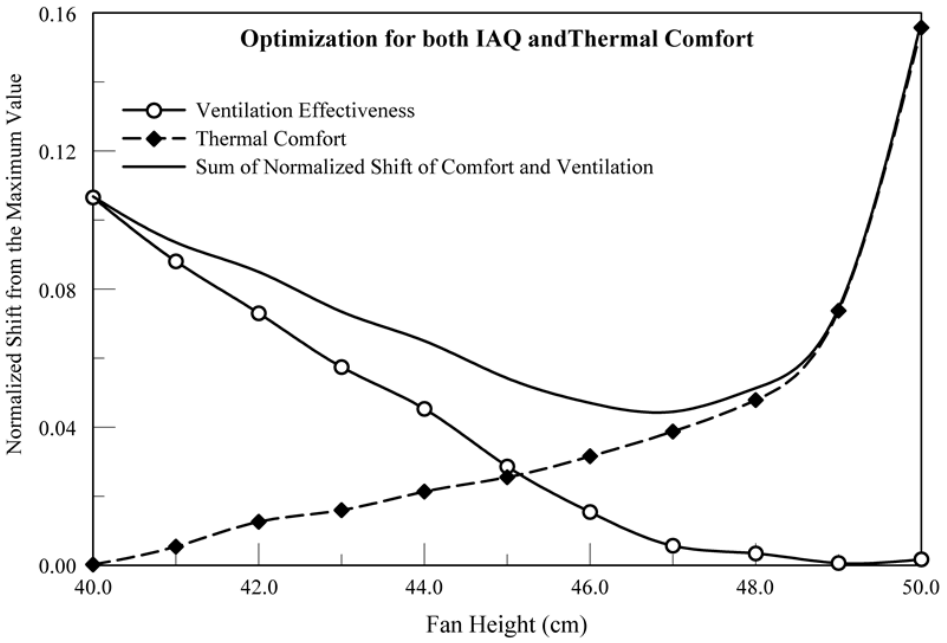

Figure 13 - the normalized shift of thermal comfort and IAQ as function of fan height at a constant total fan flow rate of 10 L/s

For the energy analysis calculations, it is assumed that the outdoor ambient air has a dry bulb temperature of 32 °C and 75% relative humidity. Therefore, the fresh air needs to be dehumidified and sensibly heated to the desired conditions. The fan of the *PV* system has a nominal power of 15 W, and the nominal power of the chair fans is 20 W. These nominal powers are then added to the electrical cost of the chiller. A typical chiller COP of 3.5 was selected for energy calculations.

The optimized chair fan assisted PV system was chosen to be compared with MV

system. The mixing ventilation system supplied air at temperature of 14 °C. The corresponding equivalent fresh air flow rate in the MV system was 13.72 L/s, 12.70 L/s, and 13.35 L/s to attain the same ventilation effectiveness at the breathing zone for case (1), (2), and (3), respectively. The energy savings that could be achieved were 16.52%, 15.86%, and 16.27% for case (1), (2), and (3) when compared to the conventional MV system. It is noticed that as the fan height increases (going from 40 cm to 50 cm) the ventilation effectiveness increases, thermal comfort decreases, and energy consumption decreases.

CHAPTER V

CONCLUSION AND RECOMMENDATIONS

This study investigates and optimizes the performance of ceiling mounted personalized ventilation (*PV*) system when assisted with chair-mounted fans. Detailed computational fluid dynamics (CFD) simulations were performed to study the velocity, temperature, and CO_2 fields around the microclimate of the occupant. The CFD model was integrated with a bioheat model to determine the corresponding segmental skin temperature and local and overall comfort and sensation. The CFD model was validated experimentally using a thermal manikin in a climatic chamber. Segmental skin temperature, velocity field, and CO_2 field were validated experimentally. The predicted values and the measured values showed good agreement.

The validated CFD model was used to optimize the height of chair-fan and the fan flow rate for the best combination of indoor air quality and thermal comfort. The chair fans configuration to achieve best thermal comfort and best IAQ occurred at different fan heights. The optimal fan height and flow rate for best thermal comfort were 40 cm above floor level and 10 L/s, respectively. However, the optimal fan height and flow rate for best air quality were found to be 50 cm above the floor level and 10 L/s,

respectively. At this configuration, the chair-mounted-fans were able to reduce the thermal plumes and improve the performance of the *PV* system by nearly doubling thermal comfort and ventilation effectiveness. The use of chair mounted fans permitted achieving energy savings up to 17% when compared with conventional mixing ventilation system.

The localized HVAC system was studied to obtain the optimal height and flow rate of the fan. The aim of this part is to find the best (optimal) combination of fan height and flow rate to attain best IAQ and thermal comfort at minimum energy consumption. Two main criteria are to be considered in every energy efficient-healthy building design, (i) providing good indoor air quality and (ii) maintaining good thermal comfort. In addition to these parameters, the proposed system tends to decrease the electrical cost. Ceiling mounted personalized systems are considered one of the promising solutions to solve ducting problems, chair fans have proved to be very effective in enhancing the performance of the ceiling mounted *PV* system. Installing chair fans to control the human convective thermal plume has shown a remarkable enhancement in terms of indoor air quality and thermal comfort. When operating the chair fans, the ventilation effectiveness (23.39%) increased by almost 2.5 times that when chair fans were turned OFF (9.31%). The fan height and fan flow rate have a dual effect on the

thermal comfort and indoor air quality, where the best IAQ is achieved at different fan configuration than that of thermal comfort. Therefore optimal height and flow rate were selected to help maintain the best combination of IAQ and thermal comfort. A peak in energy savings was achieved at the best IAQ case (fan height 50 cm and a total flow rate 10 L/s) reaching 17% when compared with mixing ventilation.

BIBLIOGRAPHY

[1] Dockery DW, Spengler JD. Personal exposure to respirable particulates and sulfates." Journal of the air pollution control association 1881; 31(2): 153-159.

[2] Cermak R, Melikov AK. Air quality and thermal comfort in an office with underfloor, mixing and displacement ventilation. International Journal of Ventilation 2006; 5(3):5.

[3] Cermak, R, Melikov AK, Forejt L, Kovar O. Performance of personalized ventilation in conjunction with mixing and displacement ventilation. HVAC&R Res. 2006; 12: 295–311.

[4] Cermak R, Melikov AK. Protection of occupants from exhaled infectious agents and floor material emissions in rooms with personalized and under floor ventilation. HVAC&R Research 2007;13(1):23-38.

[5] Kaczmarczyk J, Melikov A., Bolashikov Z, Nikolaev L, Fanger PO. Human response to five designs of personalized ventilation. International Journal of heating, Ventilation and Refrigeration Research 2006; 12 (2):367-384.

[6] Melikov AK. Personalized ventilation. Indoor Air 2004; 14(Suppl. 7):157-67.

[7] Russo JS, Dang TQ, Khalifa HE. Computational analysis of reduced-mixing personal ventilation jets. Building and Environment 2009; 44:1559 - 1567.

[8] Yang B, Sekhar C, Melikov AK. Ceiling mounted personalized ventilation system in hot and humid climate - An energy analysis. Energy and Buildings 2010;42:2304-2308.

[9] Bolashikov ZD, Melikov AK, Krenek M. Control of the free convective flow around the human body for enhanced inhaled air quality: Application to a seat-incorporated personalized ventilation unit. HVAC&R Research 2010; 16(2):161-188.

[10] Bolashikov ZD, Melikov AK, Krenek M. 2009, Improved performance of personalized ventilation by control of the convection flow around occupant body, ASHRAE Transactions 2009; 115(2), Paper ID: LO-09-038.

[11] Melikov AK, Kaczmarczyk J. Indoor air quality assessment by a breathing thermal manikin. Indoor Air 2007; 17(1):50-59.

[12] Melikov AK. Human body micro-environment: the benefits of controlling airflow interaction. Building and Environment 2015. doi:10.1016/j.buildenv.2015.04.010.

[13] Yang B. Thermal Comfort and Indoor Air Quality Evaluation of a Ceiling Mounted Personalized Ventilation System Integrated with an Ambient Mixing Ventilation System, PhD thesis. National University of Singapore. Singapore; 2009.

[14] Yang B, Chandra S, Melikov A. Ceiling mounted personalized ventilation system in hot and humid climate e an energy analysis. Energy Buildings 2010; 42:2304-8.

[15] Makhoul A, Ghali K, Ghaddar N. Low-mixing coaxial nozzle for effective personalized ventilation. Indoor and Built Environment, 2015;24 (2): 225-243.

[16] Makhoul A. Ceiling-mounted fresh air personalized ventilator for occupant controlled microenvironment. Proceedings of the ASME 2012 International Mechanical Engineering Congress and Exposition; IMECE 2012 Volume 7: Fluids and Heat Transfer, Parts A, B, C, and D, Houston, Texas, USA, November 9–15, 2012: 1683-1693.

[17] Makhoul A, Ghali K, Ghaddar N. Desk fans for the control of the convection flow around occupants using ceilings mounted personalized ventilation. Building and Environment 2013; 59: 336-348.

[18] Khalifa HE, Janos MI, Dannenhoffer JF. Experimental investigation of reduced mixing personal ventilation jets. Building and Environment 2009; 44:1551-8.

[19] Russo JS, Dang TQ, and Khalifa HE. Computational analysis of reduced-mixing personal ventilation jets, Building and Environment 2009; 44: 1559-1567.

[20] Watanabe S, Shimomura T, Miyazaki H. Thermal evaluation of a chair with fans as an individually controlled system. Building and Environment 2009; 44:1392-8.

[21] Habchi C, Ghali K, Ghaddar N, Shihadeh A, Chair fan fan-enhanced displacement ventilation for high IAQ: Effects on particle inhalation and stratification height. Building and Environment 2005; 84: 68-79

[22] ANSYS Software: ANSYS Inc http://www.ansys.com/ .

[23] Salloum M, Ghaddar N, Ghali K. A new transient bioheat model of the human body and its integration to clothing models. Int J Thermal Sci 2007; 46: 371-84.

[24] Ghaddar N, Ghali K, Chehaitly S. Assessing thermal comfort of active people in transitional spaces in presence of air movement. Energy and Buildings 2011; 43(10):2832-2842.

[25] Zhang H, Arens E, Huizenga C, Han T. Thermal sensation and comfort models for non-uniform and transient environments: Part I: Local sensation of individual body parts. Building and Environment 2010; 45(2):380-8.

[26] Zhang H, Arens E, Huizenga C, Han T. Thermal sensation and comfort models for non-uniform and transient environments: Part II: local comfort of individual body parts. Building and Environment 2010; 45(2):389-98.

[27] Zhang H, Arens E, Huizenga C, Han T. Thermal sensation and comfort models for non-uniform and transient environments: Part III: whole-body sensation and comfort. Building and Environment 2010; 45(2):399-410.

[28] Makhoul A, Ghali K, Ghaddar N, Chakroun W. Investigation of particle transport in offices equipped with ceiling-mounted personalized ventilators. Building and Environment 2013; 63:97-107.

[29] Makhoul A, Ghali K, Ghaddar N. The energy saving potential and the associated thermal comfort of displacement ventilation systems assisted by personalized ventilation. Indoor Built Environ 2013; 22:508-19.

[30] Dougan D, Damiano L. CO_2-Based demand control ventilation. ASHRAE Journal 2004; 47:52-54

[31] ANSI/ASHRAE. Standard 62.1-2013, Ventilation for Acceptable Indoor Air Quality. Atlanta: American Society of Heating, Air- Conditioning and Refrigeration Engineers, Inc; 2013.

[32] Schell M, Inthout D. Demand control ventilation using CO_2." ASHRAE Journal 2001;2:1-6 Available: https://airtest.com/support/reference/article2.pdf.

[33] Epoxy Thermal Manikin. INSTRUMENTS FOR TEXTILE & BIOPHYSICAL TESTING. Seattle, WA, [Online]. Available: http://www.thermetrics.com/sites/default/files/product_brochures/NEWTON%20Manikin_Spec%20Sheet.pdf.

[34] ASHRAE. Handbook-fundamentals. Atlanta: American Society of Heating Air conditioning and Refrigeration Engineers, Inc; 2009.

[35] Kulkarni V, Sahoo N, Chavan S. Simulation of honeycomb screen combinations for turbulence management in a subsonic wind tunnel. J Wind Eng Indust Aerodyn 2011; 99:37-45.

[36] Newsham G, Brand J, Donnelly C, Veitch J, Aries M, Charles K. Linking indoor environment conditions to job satisfaction: a field study. Building Res Inf 2009; 37(2):129-47.

[37] Ghali K, Ghaddar N, Bizri M. The Influence of wind on outdoor thermal comfort in the city of Beirut: a theoretical and field study. Int J HVAC R Res 2011; 17(5):813-28.

[38] de Dear Cândido RJ, Lamberts R, Bittencourt L. Air movement acceptability limits and thermal comfort in Brazil's hot humid climate zone. Building Environ 2010;45(1):222-9.

[39] Huizenga C, Zhang H, Mattelaer P, Yu T, Arens EA, Lyons P. Window Performance for Human Thermal Comfort. Report submitted to National Fenestration Rating Council (2006). http://escholarship.org/uc/item/6rp85170. Accessed on April 5, 2015.